

Negative differential conductance in two-dimensional electron grids

W. Pan,^{1,a)} S. K. Lyo,¹ J. L. Reno,¹ J. A. Simmons,¹ D. Li,² and S. R. J. Brueck²

¹Sandia National Laboratories, P.O. Box 5800, Albuquerque, New Mexico 87185, USA

²Center for High Technology Materials, University of New Mexico, Albuquerque, New Mexico 87108, USA

(Received 8 July 2007; accepted 16 January 2008; published online 5 February 2008)

Negative differential conductance has been observed in grid-shaped surface superlattices, realized in a high mobility two-dimensional electron system. The current-voltage characteristics vary with the modulation strength, indicating that the two-dimensional electronic transport properties can be manipulated in a controllable way. Theoretical modeling yields reasonable agreement with the experimental data. © 2008 American Institute of Physics. [DOI: 10.1063/1.2840996]

In a periodic structure of electron potential, under an external electric field E , if an electron can reach the boundary of the Brillouin zone (BZ) without being scattered, it undergoes Bragg reflection, passing back into the BZ on the opposite side. This results in a high frequency (f) oscillation of electron, i.e., Bloch oscillation (BO), at $f=eEd/h$, where d is the period of the potential, e is the electron charge, and h is Planck's constant. When the magnitude of electric field and the period of potential are properly chosen, the Bloch frequency can fall in the terahertz region. Proposed about 80 years ago,¹ recently, BO has gained a renewed interest, as a Bloch oscillator can be utilized as a solid-state, electrically biased, frequency-tunable terahertz source and detector.

So far, work on BO has mainly been carried out in vertical quantum well superlattice structures.^{2–10} On the other hand, a surface superlattice patterned in a two-dimensional electron system (2DES) has long been proposed as an alternative device structure to generate BO.^{11–16} A surface superlattice has three-dimensional quantization, as opposite to the conventional vertical quantum well superlattice.¹³ As a result, gaps in the energy spectrum exist in all three dimensions. This provides the possible existence of BO at relatively moderate electric field. It has also been shown that,^{13,16} in surface superlattices, the electron-optical phonon scattering, one of the limiting mechanisms in achieving BO in the terahertz range in vertical superlattice, can be completely suppressed, and electrically generated BO can become possible. Furthermore, compared to a vertical superlattice, a surface superlattice offers other various advantages, for example, easy device fabrication and multiple fundamental frequencies. It can also fully utilize the benefit of long coherent transport time achieved in high mobility 2DES. To date, however, very few studies of BO in surface superlattices have been reported.

In this paper, we report the experimental observation of negative differential conductance (NDC) in surface superlattices, one of the signatures of BO. Two devices with varying coupling strengths are studied and, in both samples, NDC is observed. Our theoretical simulation, based on an energy relaxation-time approximation and a microscopic short-range elastic scattering model for the momentum relaxation,¹⁷ yields reasonable agreement with the experimental data.

To minimize electron scattering by residual impurities and to achieve long coherent transport time, the starting ma-

terial is a high mobility 2DES realized in a GaAs quantum well (QW) of width 300 Å. The low temperature density and mobility of 2DES are $n \sim (2-3) \times 10^{11} \text{ cm}^{-2}$ and $\mu > 1 \times 10^6 \text{ cm}^2/\text{V s}$, respectively, before patterning. After the patterning, the electron mobility was reduced somewhat. Two specimens (samples A and B), cut from two wafers, were studied. The growth structure for the two wafers is basically the same, except that in wafer A, the quantum well is 200 nm below the surface, while in wafer B is 150 nm below. A low frequency lock-in technique was used to measure the low-temperature magnetoresistance (R_{xx}) and a Keithley K236 source meter was used to supply the source-drain dc bias (V_{dc}) and to measure the source-drain current (I_{ds}).

In our experiments, a surface superlattice was realized in a two-dimensional (2D) electron grid device. The 2D electron grid was fabricated by depositing a periodic 2D metal grid on the surface of QW samples. The metal consists of Ti/Au, about 80 nm thick. A scanning electron microscopy (SEM) picture of metal grid is shown in the inset of Fig. 1(a). The pitch of the metal grid is ~ 350 nm and the diameter of the holes is ~ 150 nm. To achieve this large-area nanometer scale patterning, the interferometric lithography technique was employed.¹⁸ In experiments, the grid devices were cooled in darkness to 4 K and a low temperature illumination by a red-light-emitting diode was used to realize the low temperature density and mobility. During each cooldown, the sample, including the metal grid, was grounded. Due to the different thermal expansion coefficients

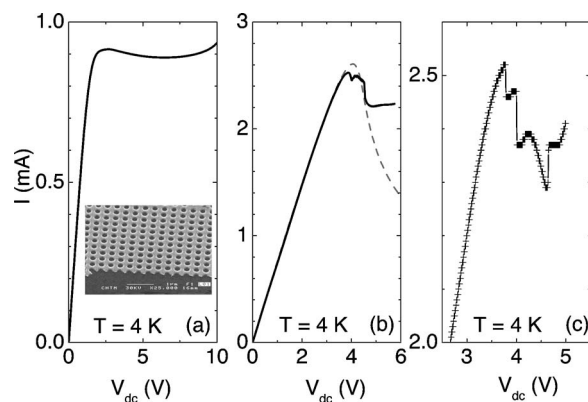


FIG. 1. (a) I - V trace in sample A. (b) I - V trace in sample B. Gray dash line represents the theoretical data. (c) Zoom-in plot of I - V trace in a different cooldown for sample B. Jumps in current in the negative differential conductance regime are apparent.

^{a)}Electronic mail: wpan@sandia.gov.

of the metal and the GaAs/AlGaAs semiconductor, the mechanical stress induces a two-dimensional electron potential modulation of the 2DES. To characterize this modulation, we have adopted well-documented methods¹⁹ by measuring R_{xx} . Similar to previous results, a positive magnetoresistance near zero magnetic (B) field and the commensurate oscillations were observed. From the saturation B field of the positive magnetoresistance,²⁰ we estimated that the modulation amplitude is $\sim 3\%$ of the Fermi energy (E_F) (or ~ 0.3 meV) for sample A, and 15% (~ 1 meV) for sample B. To compare, in a reference sample without patterning neither positive magnetoresistance nor commensurate oscillation was observed in R_{xx} .

Current-voltage (I - V) measurement was carried out at 4 K, using a Keithley K236 source meter. In Fig. 1, the I - V curves of samples A and B are shown. At small V_{dc} , both devices show Ohmic behavior, and the corresponding resistance is $\sim 1500 \Omega$ for sample A and $\sim 3000 \Omega$ for sample B. These resistances include wire and contact resistance in addition to the sample resistance. In sample A [Fig. 1(a)], I_{ds} reaches a maximal value of ~ 0.92 mA at $V_{dc} \sim 2.7$ V, and then decreases as V_{dc} continues to increase, reaching a local minimum of 0.89 mA around ~ 6.5 V. After this, I_{ds} increases again with increasing V_{dc} . In other words, a negative differential conductance is observed between ~ 2.7 and ~ 6.5 V. In sample B, where a stronger modulation is achieved, again, a NDC is observed. In Figs. 1(b) and 1(c), we show the I - V curves from two different cooldowns. Two features are worthwhile emphasizing: (1) the maximal current is significantly higher than that in sample A, ~ 2.5 mA at $V_{dc} \sim 3.8$ V; (2) more complex structures are observed in the NDC regime. In particular, in Fig. 1(c), three current jumps are observed at $V_{dc} \sim 3.8$, 4.0 , and 4.6 V.

The observation of NDC is exciting. Recall that NDC was predicted and taken as the evidence of Bloch oscillations in vertical quantum well superlattices by Esaki and Tsu in their original paper.² In surface superlattices, it was shown¹¹⁻¹⁵ that the bend over in the I - V curve could also be due to the onset of Bloch oscillations, where electrons are able to cycle many times through the reduced Brillouin zone before a scattering event can happen.¹³ Thus, the observed NDC may indeed represent the evidence of electron self-oscillations in our 2D electron grids. Furthermore, the I - V curves show different characteristics in the two samples, indicating that the I - V characteristics and the 2D electronic transport properties can be manipulated by adjusting the structure. Finally, we note the observation of current jumps in the NDC region in our GaAs surface superlattice. Similar current jumps have been observed in InGaAs/InAlAs vertical superlattices²¹ and in InAs/AlSb resonant-tunneling diodes,²² and were attributed to self-rectification of the electron oscillation.²³

Of course, other mechanisms such as the formation of high electric-field domains and the so-called thermal runaway, can also induce an apparent NDC. It has been shown that stationary or propagating domains can form in 2D structures.²⁴ In this regard, it is possible that current jumps might be produced as the domain boundary moves through the interface fluctuations induced by surface superlattice.²⁵ On the other hand, the two-dimensional nature of conducting channels should help to stabilize the electrical field in surface superlattices and prevent the formation of high electric-field domains. It is interesting to study in future experiments

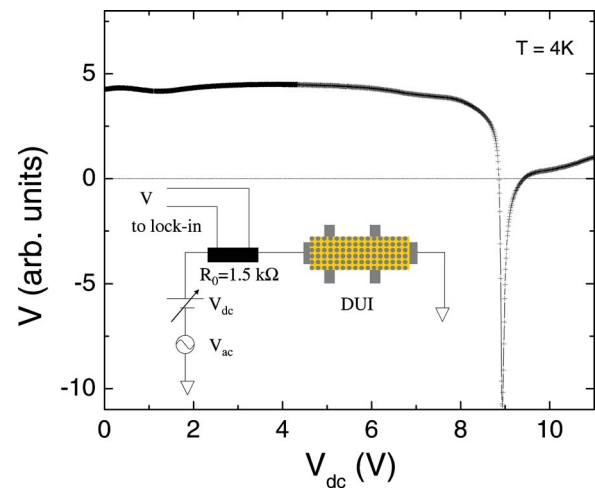


FIG. 2. (Color online) Differential measurement for verifying the thermal runaway origin of the observed NDC. The inset shows the experimental setup. R_0 is a thin-film resistor.

whether the current jump observed in our device is related to the domain formation.

To experimentally eliminate the possibility of thermal runaway origin, we employ a “differential” measurement setup (as shown in the inset of Fig. 2), where a thin film resistor of constant value $R_0 = 1500 \Omega$ is connected in series with the two-dimensional electron grid (sample B). A small alternating current bias (V_{ac}) is added to V_{dc} . The voltage measured by a lock-in amplifier is given by $V = V_{ac}R_0/(R_0 + r)$, where $r = dV/dI$ is the differential resistance of the two-dimensional electron grid. Here, we have omitted the wire and contact resistance, since they are relatively small compared to $|r|$ in the NDC region. If the observed NDC is of thermal runaway origin, r is always positive. Consequently, V is expected to be positive, at any V_{dc} . On the other hand, if r is caused by dynamic localization through BO, then $r < 0$. In the case of $|r| \gg R_0$, V is expected to be negative in the NDC region. In Fig. 2, we show V as a function of V_{dc} . At small V_{dc} , V is nearly constant, consistent with the observation in Fig. 1 that our electron grid is Ohmic at small V_{dc} . Starting from $V_{dc} \sim 8$ V, V begins to decrease. At $V_{dc} \sim 8.9$ V, V becomes negative.²⁶ The observation of negative V shows that, indeed, the observed NDC is not a result of thermal effects.

To help understand the physical origin of NDC, a theoretical study was carried out for sample B with 15% modulation. We first calculate the energy band structures. In our device with a periodic in-plane potential modulation, the original modulation-free single conduction band is folded into many Bloch minibands with small miniband gaps. Surprisingly, each miniband can be represented by a few-component cosine function (similar to Esaki’s band) with negligible contributions from higher harmonics. To calculate the I - V characteristic, we use a model similar to that by Gerhardt,¹⁷ except that our model treats a degenerate 2D electron gas and assumes that the matrix element for elastic scattering is independent of the initial and final momentum (relevant to short-range impurity potentials), thereby treating 2D interband scattering with an equal weight. Also, in our calculation, a simplified model, where the electron potential modulation is one-dimensional in the field direction, is used. We believe that the physics for a qualitative understanding

should essentially be the same as in the two-dimensional electron grid. Details of our theoretical calculations will be published elsewhere. The theoretical result is shown in Fig. 1(b) by the gray dash line. Overall, the theoretical result is in a reasonable agreement with the experimental data, except that the decrease of current in the NDC regime is steeper than that of the experimental data. We also note here that the effective current cross section employed in theoretical calculations is smaller than the geometric cross section of real device by a factor of a few, and the electron scattering rate is larger than that deduced from the mobility. Those discrepancies probably are related to the assumptions of (1) a one-dimensional model and (2) field-independent inelastic scattering rate we made in the calculation. Finally, for a self-consistent check, for a parabolic band in the absence of periodic potential modulation, our model yields linear field dependence of current and therefore no NDC.

In conclusion, we have observed a NDC in two-dimensional electron grid devices, and in one sample, several current jumps in the NDC region. Our theoretical modeling yields reasonable agreement with the experimental data. The observed NDC may represent the evidence of Bloch oscillation in our two-dimensional electron grids.

We are grateful to Mark Lee for suggesting to us the measurement in Fig. 2, and Mike Wanke for bringing our attention to Ref. 24. We thank Denise Tibbetts for her excellent technical assistance. This project was supported, in part, by LDRD and DOE/BES at Sandia National Laboratories. Sandia is a multiprogram laboratory operated by Sandia Corporation, a Lockheed Martin company, for the United States Department of Energy's National Nuclear Security Administration under Contract No. DE-AC04-94AL85000. The facilities of the NSF-sponsored NNIN node at the University of New Mexico were used for the fabrication.

- ¹F. Bloch, *Z. Phys.* **52**, 555 (1928).
- ²L. Esaki and R. Tsu, *IBM J. Res. Dev.* **14**, 61 (1970).
- ³K. K. Choi, B. F. Levine, R. J. Malik, J. Walker, and C. G. Betha, *Phys. Rev. B* **35**, 4172 (1987).
- ⁴J. Bleuse, G. Bastard, and P. Voisin, *Phys. Rev. Lett.* **60**, 220 (1988).
- ⁵E. E. Mendez, F. Agullo-Rueda, and J. M. Hong, *Phys. Rev. Lett.* **60**, 2426 (1988).
- ⁶A. Sibille, J. F. Palmier, H. Wang, and F. Mollot, *Phys. Rev. Lett.* **64**, 52 (1990).
- ⁷F. Beltram, F. Capasso, D. L. Sivco, A. L. Hutchinson, S. N. G. Chu, and A. Y. Cho, *Phys. Rev. Lett.* **64**, 3167 (1990).
- ⁸K. Uttertrainer, B. J. Keay, M. C. Wanke, S. J. Allen, D. Leonard, G. Medeiros-Ribeiro, U. Bhattacharya, and M. J. W. Rodwell, *Phys. Rev. Lett.* **76**, 2973 (1996).
- ⁹Y. Shimada, N. Sekine, and K. Hirakawa, *Appl. Phys. Lett.* **84**, 4926 (2004).
- ¹⁰T. Feil, H.-P. Tranitz, M. Reinwald, and W. Wegscheider, *Appl. Phys. Lett.* **87**, 212112 (2005).
- ¹¹H. Sakaki, K. Wagatsuma, J. Hamasaki, and S. Saito, *Thin Solid Films* **36**, 497 (1976).
- ¹²G. J. Iafrate, D. K. Ferry, and R. K. Reich, *Surf. Sci.* **113**, 485 (1982).
- ¹³R. Reich, Ph.D. thesis, Colorado State University at Fort Collins, 1982.
- ¹⁴G. Bernstein and D. K. Ferry, *J. Vac. Sci. Technol. B* **5**, 964 (1987).
- ¹⁵K. Ismail, W. Chu, D. A. Antoniadis, and H. I. Smith, *Appl. Phys. Lett.* **54**, 460 (1989).
- ¹⁶I. A. Dmitriev and R. A. Suris, *Semiconductors* **35**, 212 (2001).
- ¹⁷R. F. Gerhardt, *Phys. Rev. B* **48**, 9178 (1993).
- ¹⁸S. C. Lee and S. R. J. Brueck, *J. Vac. Sci. Technol. B* **22**, 1949 (2004).
- ¹⁹D. Weiss, M. L. Roukes, A. Menschig, P. Grambow, K. von Klitzing, and G. Weimann, *Phys. Rev. Lett.* **66**, 2790 (1991).
- ²⁰P. H. Benton, E. S. Alves, P. C. Main, L. Eaves, M. W. Dellow, M. Henini, O. H. Hughes, S. P. Beaumont, and C. D. W. Wilkinson, *Phys. Rev. B* **42**, 9229 (1990).
- ²¹E. Schomburg, R. Scheuerer, S. Brandl, K. F. Renk, D. G. Pavel'ev, Yu. Koschurinov, V. Ustinov, A. Zhukov, A. Kovsh, and P. S. Kop'ev, *Electron. Lett.* **35**, 1491 (1999).
- ²²E. R. Brown, J. R. Soderstrom, C. D. Parker, L. J. Mahoney, K. M. Molvar, and T. C. McGill, *Appl. Phys. Lett.* **58**, 2291 (1991).
- ²³H. C. Liu, *Appl. Phys. Lett.* **53**, 485 (1988).
- ²⁴B. K. Ridley, *Semicond. Sci. Technol.* **3**, 542 (1988).
- ²⁵K. J. Luo, K.-J. Friedland, H. T. Grahn, and K. H. Ploog, *Phys. Rev. B* **61**, 4477 (2000).
- ²⁶Due to the load resistance R_0 , the NDC region is pushed to higher V_{dc} , compared to Fig. 1(b).